

RESEARCH ARTICLE**Structured Singular Value of a Repeated Complex Full-Block Uncertainty**Talha Mushtaq¹ | Diganta Bhattacharjee¹ | Peter Seiler² | Maziar S. Hemati¹¹Aerospace Engineering and Mechanics, University of Minnesota, Minneapolis, Minnesota, USA²Electrical Engineering and Computer Science, University of Michigan, Ann Arbor, Michigan, USA**Correspondence**

Talha Mushtaq, Email: musht002@umn.edu

Abstract

The structured singular value (SSV), or μ , is used to assess the robust stability and performance of an uncertain linear time-invariant system. Existing algorithms compute upper and lower bounds on the SSV for structured uncertainties that contain repeated (real or complex) scalars and/or non-repeated complex full-blocks. This paper presents algorithms to compute bounds on the SSV for the case of repeated complex full-blocks. This specific class of uncertainty is relevant for the input-output analysis of many convective systems, such as fluid flows. Specifically, we present a power iteration to compute the SSV lower bound for the case of repeated complex full-blocks. This generalizes existing power iterations for repeated complex scalars and non-repeated complex full-blocks. The upper bound can be formulated as a semi-definite program (SDP), which we solve using a standard interior-point method to compute optimal scaling matrices associated with the repeated full-blocks. Our implementation of the method only requires gradient information, which improves the computational efficiency of the method. Finally, we test our proposed algorithms on an example model of incompressible fluid flow. The proposed methods provide less conservative bounds as compared to prior results, which ignore the repeated full-block structure.

KEYWORDS:

Structured Singular Value, Repeated Complex Full-Blocks, Structured Uncertainty, Method of Centers

1 | INTRODUCTION

The structured singular value (SSV), or μ , is a useful metric for assessing the robust stability and performance of an uncertain linear time-invariant system with a structured uncertainty.^[1,2,3] The SSV is inversely related to the smallest structured uncertainty that destabilizes the uncertain system. Roughly, the SSV is the “gain” of the system with respect to the structured uncertainty and its inverse provides a stability margin.^[4,5] It is known that exactly computing the SSV is NP hard.^[6,7] Thus, it is a common practice to instead compute upper and lower bounds on the SSV. The upper bound provides a sufficient condition for robust stability and the lower bound for instability, respectively.^[4,5,2,8,9] However, for some specific uncertainty structures, as noted in prior works,^[2,10,11] the convex upper bound equals the SSV. Thus, for these cases, the exact SSV can be computed through the convex upper bound.

Much of the previous work has focused on structured uncertainties with a mixture of repeated (real or complex) scalars and/or non-repeated complex full-block uncertainties (see Section 2).^[4,5,2] For these common uncertainty structures, one can use the

⁰**Abbreviations:** SSV, structured singular value; PCF, plane Couette flow; I/O, input-output

methods described in prior works to compute the upper and lower bound.^[9,12,8,13] The current paper focuses on a new uncertainty structure: repeated complex full-blocks. This particular class of uncertainties consists of a single complex full-block repeated multiple times. This repeated structure naturally arises in fluid dynamics and other convective systems. Recently, SSV has emerged as a means of performing a structured input-output analysis of transitional shear flows to study instability mechanisms.^[14,15,16,17] However, Liu et al.^[14,15,16] utilize MATLAB's Robust Control Toolbox, which does not allow for repeated full-blocks. The only cases handled by MATLAB are non-repeated, complex full-blocks and the repeated (real or complex) scalars.^[18] Therefore, the numerical results in these works^[14,15,16] replace the repeated complex full-block structure with a non-repeated one, which yields conservative SSV bounds. In addition to conservatism in the bounds, accounting for the repeated uncertainty structure is important for revealing physical instability mechanisms, as will become clear in the results we present later.

In this paper, we present algorithms to compute upper and lower bounds on the SSV for a repeated complex full-block uncertainty (see Sections 3 and 4). The upper bound is computed using an interior point algorithm known as the method of centers.^[19,20] Our implementation only uses gradient (and not Hessian) information. This improves computational efficiency, which is important for any large dimensional system, such as the fluid flow example presented in our paper. The lower bound is computed by generalizing the existing power iteration algorithm described by Packard et al.^[2,13] We demonstrate the proposed algorithms on the plane Couette flow model^[14] and a simple academic example. Furthermore, we compare the SSV bounds computed from the proposed algorithms with existing methods that approximate the repeated structure with a non-repeating one. We show that the proposed algorithms not only reduce the conservatism of the bounds but also highlight the importance of incorporating the correct uncertainty structure for interpreting the underlying physical system/phenomena (see Section 5).

The symbols \mathbb{R} , \mathbb{C} , \mathbb{R}^n , \mathbb{C}^n and $\mathbb{C}^{n \times m}$ denote the sets of real numbers, complex numbers, real vectors of dimension n , complex vectors of dimension n and complex matrices of dimension $n \times m$, respectively. The $n \times n$ identity and zero matrices are denoted by I_n and 0_n , respectively. M^H and $\bar{\sigma}(M)$ are the Hermitian transpose and maximum singular value of a matrix $M \in \mathbb{C}^{n \times m}$. We use $\|\cdot\|_2$ to denote the 2-norm for vectors and the induced 2-to-2 norm for matrices. Note that $\|\cdot\|_2 = \bar{\sigma}(\cdot)$ for matrices. Also, $\|\cdot\|_F$ denotes the Frobenius norm. For $M \in \mathbb{C}^{n \times n}$, $\text{Tr}(M)$ and $\rho(M)$ are the trace and spectral radius. The notations \otimes and $\text{diag}(\cdot)$ denote the Kronecker product and block diagonal matrices, respectively. The imaginary unit is denoted as $i = \sqrt{-1}$. For $c \in \mathbb{C}$, $\text{Re}(c)$, $\text{Im}(c)$ and $\text{conj}(c)$ denote the real and imaginary parts of c , and the complex conjugate of c , respectively.

2 | BACKGROUND: STRUCTURED SINGULAR VALUE, μ

We briefly review the structured singular value μ and its connection to robust stability of dynamical systems.^[1,2,21,4] First consider the case for matrices. Specifically, let $M \in \mathbb{C}^{n \times m}$ be given along with a set of (possibly structured) complex matrices $\Delta \subseteq \mathbb{C}^{m \times n}$.

Definition 1. The structured singular value, μ_Δ , is defined as

$$\mu_\Delta(M) := \frac{1}{\min(\bar{\sigma}(\Delta) : \Delta \in \Delta, \det(I_n - M\Delta) = 0)}. \quad (1)$$

If there does not exist $\Delta \in \Delta$ such that $\det(I_n - M\Delta) = 0$, then define $\mu_\Delta(M) = 0$.

Note that $\mu_\Delta(M)$ depends on both the matrix M and the set of matrices Δ . We will typically omit the subscript Δ for simplicity when the set of matrices is clear.

The SSV is inversely related to the smallest $\Delta \in \Delta$ that causes $I_n - M\Delta$ to be singular. Singularity means there exists a nonzero vector $y \in \mathbb{C}^n$ such that $y = M\Delta y$. This is equivalent to the existence of non-zero vectors $u \in \mathbb{C}^m$ and $y \in \mathbb{C}^n$ such that $y = Mu$ and $u = \Delta y$, which provides a feedback interpretation of $\mu_\Delta(M)$ (see Remark 3.4 in Packard and Doyle^[2]). Furthermore, the SSV simplifies in two special cases:^[2]

- (i) $\mu(M) = \bar{\sigma}(M)$ for full-block uncertainties, $\Delta = \mathbb{C}^{m \times n}$,
- (ii) $\mu(M) = \rho(M)$ for repeated scalar uncertainties $\Delta = \{\delta I_v : \delta \in \mathbb{C}\}$, where $n, m = v$.

There are many known results for structured uncertainties Δ that contain block-diagonal concatenation of any number of full-blocks and repeated scalars.^[1,2,21,4] It is worth noting that if $\Delta_1 \subset \Delta_2$ then

$$\mu_{\Delta_1}(M) \leq \mu_{\Delta_2}(M). \quad (2)$$

This follows from the definition of the SSV in (1). This yields the following bound for any matrix M and block structure $\mathbf{\Delta} \subseteq \mathbb{C}^{m \times n}$:

$$\mu_{\mathbf{\Delta}}(M) \leq \bar{\sigma}(M). \quad (3)$$

Next, consider the case for LTI systems. Specifically, let $M(s)$ be a transfer function matrix of a multiple-input and multiple-output (MIMO) LTI system and $\mathbf{\Delta}$ be a set of structured LTI uncertainties. The SSV can be used to assess robustness of a feedback loop involving $M(s)$ and $\Delta(s)$. In particular, assume the feedback loop is nominally stable, i.e., stable for $\Delta(s) = 0$. Define the set of bounded, structured uncertainties as $\mathbb{B}_{\mathbf{\Delta}} := \{\Delta(s) \in \mathbf{\Delta} : \|\Delta\|_{\infty} \leq 1\}$. Then, the feedback loop is stable for all $\Delta \in \mathbb{B}_{\mathbf{\Delta}}$ if and only if $\max_{\omega} \mu(M(i\omega)) < 1$, where ω is the temporal frequency.^[1,2,21,4] This is an adaptation of the small-gain condition for the set of structured uncertainties $\mathbb{B}_{\mathbf{\Delta}}$. The SSV computations for LTI systems are often reduced to the SSV computations for a complex matrix $M(i\omega)$ on a grid of frequencies.

This paper contributes methods that can be used to compute the SSV for repeated full-block uncertainty

$$\mathbf{\Delta}_r := \{\Delta = I_v \otimes \Delta_1 : \Delta_1 \in \mathbb{C}^{m_1 \times m_1}\} \subset \mathbb{C}^{m \times m}, \quad (4)$$

where $m = v m_1$. Thus, $v = 2$ represents the same full-block uncertainty Δ_1 repeated twice: $I_2 \otimes \Delta_1 = \begin{bmatrix} \Delta_1 & 0 \\ 0 & \Delta_1 \end{bmatrix}$. The block Δ_1 is restricted to be square, as is common in the SSV literature, to simplify the presentation. The extension to non-square blocks can be made with mainly notational changes. We discuss algorithms in the subsequent sections that compute upper and lower bounds on the $\mu(M)$ for the uncertainty structure in (4).

3 | UPPER BOUND OF STRUCTURED SINGULAR VALUE

This section describes an algorithm that computes an upper bound on μ for the uncertainty structure defined in (4). We will describe the upper bound algorithm for the matrix case $M \in \mathbb{C}^{m \times m}$. We start by first noting that for each set of uncertainties $\mathbf{\Delta}$, there is a set of non-singular ‘‘commuting’’ matrices \mathbf{D} with the property that $D\Delta = \Delta D$ for any $\Delta \in \mathbf{\Delta}$ and $D \in \mathbf{D}$. For example, the set of v non-repeated full-blocks, denoted $\mathbf{\Delta}_{nr} \subset \mathbb{C}^{m \times m}$, and its corresponding commuting matrices are

$$\mathbf{\Delta}_{nr} := \{\Delta = \text{diag}(\Delta_1, \dots, \Delta_v) : \Delta_i \in \mathbb{C}^{m_i \times m_i}\}, \quad (5)$$

$$\mathbf{D}_{nr} := \{\text{diag}(d_1 I_{m_1}, \dots, d_v I_{m_v}) : d_i \in \mathbb{R}, d_i \neq 0\}. \quad (6)$$

The commuting matrices are diagonal when the uncertainty set is non-repeated. For the repeated full-block structure in (4), the commuting matrices have the following structure:

$$\mathbf{D}_r := \{S \otimes I_{m_1} : S \in \mathbb{C}^{v \times v}, \det(S) \neq 0\}. \quad (7)$$

These commuting matrices are important because $\det(I - M\Delta) = \det(I - DM D^{-1}\Delta)$. Thus, $\mu_{\mathbf{\Delta}}(M) = \mu_{\mathbf{\Delta}}(DM D^{-1})$. We can use this to strengthen the upper bound in (3):

$$\mu_{\mathbf{\Delta}}(M) \leq \min_{D \in \mathbf{D}} \bar{\sigma}(DM D^{-1}). \quad (8)$$

This is known as the D -scale upper bound. By setting $X = D^H D$, the optimization on the right hand side of (8) can be converted into a semi-definite program (technically a generalized eigenvalue problem) as follows:^[2,4]

$$\begin{aligned} & \min_{X = X^H \in \mathbb{C}^{m \times m}, \zeta \in \mathbb{R}} \zeta \\ & \text{subject to: } M^H X M < \zeta X, X > 0. \end{aligned} \quad (9)$$

Then, the upper bound is computed as $\alpha = (\zeta)^{1/2}$ and the corresponding scale as $D = X^{1/2}$. Therefore, there is an implicit constraint that $\zeta \geq 0$, which arises naturally during the derivation of constraints in (9) (see Packard and Doyle^[2] for details). The optimization problem (9) can be solved using several existing methods such as method of centers, interior-point methods for linear fractional programming, and primal-dual methods.^[20,22,23] These methods are efficient for moderate-sized problems but can be computationally costly for larger dimensioned problems. Specifically, primal-dual methods tend to be slower because they require second-order schemes to solve (9). Certainly, there are faster algorithms that utilize a weaker bound, i.e., $\bar{\sigma}(DM D^{-1}) \leq \|DM D^{-1}\|_F$, which is often sufficient for most large-dimensioned problems. In this case, an upper bound for a given matrix M becomes

$$\mu_{\mathbf{\Delta}}(M) \leq \min_{D \in \mathbf{D}} \|DM D^{-1}\|_F. \quad (10)$$

See Appendix A for a fast algorithm for computing an upper bound of the form (10) for $D \in \mathbf{D}_r$, i.e., the repeated full-blocks case. However, using a weaker bound yields conservative estimates of the upper bounds, which can result in large gaps between upper and lower bounds. The goal of this paper is to present an efficient algorithm that would yield the least conservative upper bounds for $\Delta \in \mathbf{\Delta}_r$. Thus, we will implement the method of centers for upper bound calculations, since it is a relatively fast first-order method with good convergence properties.^[19] First, we will briefly summarize an existing upper bound method for the uncertainty structure $\mathbf{\Delta}_{nr}$, which we will use later to compare with the upper bounds obtained for $\mathbf{\Delta}_r$.

3.1 | Standard Osborne's Method: Non-Repeated Complex full-blocks

Osborne's iteration can be used to efficiently solve the optimization problem in the right-hand side of (10) for specific block structures.^[24] For example, a version of Osborne's iteration can be applied to the structure $\mathbf{\Delta}_{nr}$ with scalings \mathbf{D}_{nr} . Let $D_i \in \mathbf{D}_{nr}$ denote a scaling with $d_j = 1$ for all $j \neq i$. For example, if $i = 1$ then d_1 is a variable and $d_j = 1$ for $j \neq 1$. In addition, partition M into $m_i \times m_j$ sub-blocks, denoted \hat{M}_{ij} , consistent with the block dimensions in $\mathbf{\Delta}_{nr}$. Then, the Frobenius norm can be written as

$$\|D_i M D_i^{-1}\|_F^2 = \sum_{r=1, r \neq i}^v \frac{1}{d_i^2} \|\hat{M}_{ri}\|_F^2 + d_i^2 \|\hat{M}_{ir}\|_F^2. \quad (11)$$

The optimal value d_i^* that minimizes (11) is given by

$$d_i^* = \left(\frac{\sum_{r=1, r \neq i}^v \|\hat{M}_{ri}\|_F^2}{\sum_{r=1, r \neq i}^v \|\hat{M}_{ir}\|_F^2} \right)^{1/4}. \quad (12)$$

Each d_i^* is computed from (12) using M and the corresponding matrix D^* is determined. Then, the cost is obtained as $\|M^{[2]}\|_F^2$, where $M^{[2]} = D^* M D^{*-1}$. The new D -scale is then computed from $M^{[2]}$ and the corresponding new cost is determined. Thus, the iteration proceeds by updating the matrix as $M^{[k]} = (D^*)^{[k]} M (D^{*-1})^{[k]}$ and computing the corresponding $(D^*)^{[k]}$ until $\|M^{[k]}\|_F^2$ has converged. The final D -scale is denoted by D_{nr}^* after all the iterations. Osborne showed that the iterative method always converges to the optimal solution of $\min_{D \in \mathbf{D}} \|DM D^{-1}\|_F$ for the uncertainty $\mathbf{\Delta}_{nr}$ with $m_i = 1$.^[24]

3.2 | Method of Centers: Repeated Complex Full-Blocks

In this section, we discuss the method of centers approach for solving the generalized eigenvalue problem (9) for the case when $\Delta \in \mathbf{\Delta}_r$ and, consequently, $D \in \mathbf{D}_r$. In this case, we have $X = (S \otimes I_{m_1})^H (S \otimes I_{m_1}) = S^H S \otimes I_{m_1} = R \otimes I_{m_1}$, where $R := S^H S$. Therefore, the generalized eigenvalue problem (GEVP) in (9) becomes

$$\begin{aligned} & \min_{R=R^H \in \mathbb{C}^{v \times v}, \zeta \in \mathbb{R}} \zeta \\ & \text{subject to: } M^H (R \otimes I_{m_1}) M < \zeta (R \otimes I_{m_1}), \quad R > 0. \end{aligned} \quad (13)$$

Since a feasible R for (13) is scale-invariant (i.e., for a feasible R , any cR with $c > 0$ is also feasible), we will replace the $R > 0$ constraint in (13) with $\frac{1}{\gamma} I_v \leq R \leq \gamma I_v$ to prevent solutions from becoming ill-conditioned, where $\gamma > 0$ and γ^2 is the (specified) condition number of R . Therefore, we numerically implement the following GEVP:

$$\begin{aligned} & \min_{R=R^H \in \mathbb{C}^{v \times v}, \zeta \in \mathbb{R}} \zeta \\ & \text{subject to: } M^H (R \otimes I_{m_1}) M < \zeta (R \otimes I_{m_1}), \\ & \quad \frac{1}{\gamma} I_v \leq R \leq \gamma I_v. \end{aligned} \quad (14)$$

The method of centers is an interior-point algorithm that solves for the analytic center of linear matrix inequality (LMI) constraints, given an initial feasible solution.^[19,20] Specifically in (14), we are minimizing the largest generalized eigenvalue ζ of the matrix pair $(M^H (R \otimes I_{m_1}) M, (R \otimes I_{m_1}))$. The algorithm utilizes a gradient descent approach, which involves computing the stepping direction towards an optimal R and the smallest $\zeta \geq 0$ satisfying the LMI constraints. To this end, the directional derivative is computed using a barrier-function for symmetric positive semi-definite matrices, i.e., $J(R) = -\log \det(R)$.

Next, we will compute the derivative of $J(R)$. Let $r_{ij} \in \mathbb{C}$ denote the (i, j) entry of R . Since R is Hermitian, the diagonal entries are real, i.e., $r_{ii} \in \mathbb{R}$. Note that the derivative of the barrier function is calculated with respect to the real and imaginary parts of each (i, j) element of R . Therefore, each matrix variable in (14) is decomposed as a summation in terms of its basis as

$R = \sum_{i,j} r_{ij} R_{ij}$, where R_{ij} is the standard basis for $\mathbb{R}^{v \times v}$. Then, the barrier function and its derivative with respect to r_{ij} are given by

$$J(R) = -\log \det(L_1) - \log \det(L_2) - \log \det(L_3), \quad (15)$$

$$\begin{aligned} \frac{\partial J(R)}{\partial r_{ij}} &= -\zeta \text{Tr} \left((R_{ij} \otimes I_{m_1})^T L_1^{-1} \right) \\ &\quad + \text{Tr} \left((R_{ij} \otimes I_{m_1})^T M L_1^{-1} M^H \right) \\ &\quad + \text{Tr} \left(R_{ij}^T L_2^{-1} \right) - \text{Tr} \left(R_{ij}^T L_3^{-1} \right), \end{aligned} \quad (16)$$

where $L_1 = \zeta(R \otimes I_{m_1}) - M^H(R \otimes I_{m_1})M$, $L_2 = \gamma I_v - R$ and $L_3 = R - \frac{1}{\gamma} I_v$. To further simplify the expression in (16), it will be useful to block partition a given matrix $H \in \mathbb{C}^{m \times m}$, where $(H)_{ij} \in \mathbb{C}^{m_1 \times m_1}$ denotes the (i, j) block for all $i, j = 1, \dots, v$.¹ Thus, $\text{Tr}((R_{11} \otimes I_{m_1})^T L_1^{-1}) = \text{Tr}((L_1^{-1})_{11})$, which can be generalized to any (i, j) , i.e., $\text{Tr}((R_{ij} \otimes I_{m_1})^T L_1^{-1}) = \text{Tr}((L_1^{-1})_{ij})$. The other terms in (16) can be simplified in a similar manner and we eventually obtain the following expression:

$$\begin{aligned} \frac{\partial J(R)}{\partial r_{ij}} &= -\zeta \text{Tr} \left((L_1^{-1})_{ij} \right) + \text{Tr} \left((M L_1^{-1} M^H)_{ij} \right) \\ &\quad + (L_2^{-1})_{ij} - (L_3^{-1})_{ij}. \end{aligned}$$

Thus, the derivative $\Phi_R := \partial J / \partial R$ can be expressed as

$$\Phi_R = -\zeta \Gamma(L_1^{-1}) + \Gamma(M L_1^{-1} M^H) + L_2^{-1} - L_3^{-1},$$

where $\Gamma : \mathbb{C}^{m \times m} \rightarrow \mathbb{C}^{v \times v}$ is a block-trace operator such that the (i, j) entry of $\Gamma(H)$ is equal to $\text{Tr}((H)_{ij})$. An overall summary of the proposed method for upper bound calculation using the method of centers is provided in Algorithm 1.

It is possible to compute the convergence properties of the algorithm using a second-order primal dual method, which utilizes the Hessian of the LMIs. However, second-order methods are computationally expensive, especially when the system has a large dimension. For practical purposes, it is computationally efficient to first calculate the lower bounds β using the power-iteration (see Section 4 for details) and then compute the upper bounds α . Despite the inherent convergence issues of the power-iteration,^[8,13] it is always possible to obtain a perturbation, which would result in a valid lower bound of SSV. Then, the gap between the upper and lower bound can be studied to assess the viability of the solution. Therefore, we terminate our algorithm when the upper bounds α are within a certain desired ratio of the lower bounds β , i.e., $\frac{\alpha}{\beta} \leq p$, where $p > 1$ is the chosen bound of the ratio. For example, we can choose $p = 1.05$ as the desired ratio for our algorithm to get the bounds within 5% of one another. It is important to note that for the cases where the upper bounds fail to satisfy p , we take the next best upper bound that will result in a ratio closest to p . Certainly, if the gap is too large, e.g., $2p < \frac{\alpha}{\beta}$, then either the lower bound has not converged or possibly the upper bound is not exact. Additionally, a simple initial estimate of R for Algorithm 1 is $R = \text{diag}((d_1^*)^2, \dots, (d_v^*)^2)$, where d_i^* is computed from the Osborne's iteration, which we will use in Section 5 for the results. It should be noted that a variant of Algorithm 1 can be conceived for $\Delta \in \mathbf{\Delta}_{\text{nr}}$ by restricting R to be diagonal with real entries.

4 | LOWER BOUND OF STRUCTURED SINGULAR VALUE

In this section, we give details on the computation of SSV lower bound for $\Delta \in \mathbf{\Delta}_r$ using the generalized power iteration algorithm. The algorithm follows the same steps as the standard power iteration commonly used for complex uncertainties given in Packard and Doyle^[2] but with slightly modified equations. We will show that the generalized version reduces to the standard algorithm for the commonly used complex uncertainties as a special case. Thus, the standard power iteration for the repeated scalars and full-block uncertainties is described first so the extension to the generalized version will be clear.

¹For $m = v$, $(H)_{ij} \in \mathbb{C}$ is the (i, j) scalar element of H

Algorithm 1 Upper Bound: Method of Centers

- 1: (Initialization) Choose any feasible $\theta \ll 1$, $\epsilon \ll 1$ and $r_{\text{cond}} > 0$. Set $R = \text{diag}((d_1^*)^2, \dots, (d_v^*)^2)$, $\alpha = \bar{\sigma}((R \otimes I_{m_1})^{1/2} M (R \otimes I_{m_1})^{-1/2})$ and $\lambda = \alpha + \epsilon$. Choose a suitable $p > 1$ and maximum number of iterations k_m .
- 2: **while** $\frac{\alpha}{\beta} \geq p$ & $k \leq k_m$ **do**
- 3: Set $\lambda = (1 - \theta)\alpha + \theta\lambda$ and $l = 1$.
- 4: **while** $l \leq 2$ **do**
- 5: $L_1 = \lambda^2(R \otimes I_{m_1}) - M^H(R \otimes I_{m_1})M$, $L_2 = \gamma I_v - R$ and $L_3 = R - \frac{1}{\gamma} I_v$.
- 6: $\Phi_R = \Gamma(M L_1^{-1} M^H) - \lambda^2 \Gamma(L_1^{-1}) + L_2^{-1} - L_3^{-1}$.
- 7: Obtain the step-size δ through a line search.
- 8: Set $R = R - \delta \Phi_R$, $l = l + 1$.
- 9: **end while**
- 10: Set $D = (R \otimes I_{m_1})^{1/2}$, $k = k + 1$.
- 11: Then, $\alpha = \sqrt{\lambda_{\max}(D^{-H} M^H (R \otimes I_{m_1}) M D^{-1})}$.
- 12: **end while**
- 13: The upper bound: α

4.1 | Standard Power Iteration: Repeated Scalars and Full Blocks

This section briefly summarizes the SSV power iterations for complex uncertainties described in Packard and Doyle.^[2] We will consider a problem with a given $M \in \mathbb{C}^{m \times m}$ and a block structure with one repeated scalar and one full-block:

$$\mathbf{\Delta} := \left\{ \Delta = \begin{bmatrix} \delta_1 I_{m_1} & 0 \\ 0 & \Delta_2 \end{bmatrix} : \delta_1 \in \mathbb{C}, \Delta_2 \in \mathbb{C}^{m_2 \times m_2} \right\}$$

where, for consistency among the dimensions, we have $m = m_1 + m_2$. The power iteration will be described for this particular block structure. The generalization to other uncertainty block structures with arbitrary numbers of repeated scalars or full-blocks will be clear.

Note that any particular $\Delta \in \mathbf{\Delta}$ such that $\det(I_n - M\Delta) = 0$ yields a lower bound $\mu(M) \geq \frac{1}{\bar{\sigma}(\Delta)}$. The exact value of $\mu(M)$ is computed by finding the “smallest” $\Delta \in \mathbf{\Delta}$ such that $\det(I_n - M\Delta) = 0$. The determinant condition is equivalent to finding $\Delta \in \mathbf{\Delta}$ and non-zero vectors $y \in \mathbb{C}^m$ and $u \in \mathbb{C}^m$ such that $y = Mu$ and $u = \Delta y$. The power iteration is an efficient method to find uncertainties $\Delta \in \mathbf{\Delta}$ that satisfy the determinant condition. The power iteration does not, in general, find the smallest uncertainty and hence it only yields a lower bound on $\mu(M)$. However, these lower bounds are often accurate in practice.^[2] Moreover, the particular uncertainty returned by the power iteration can be studied further for insight.

To describe the power iteration, consider vectors $a, z, b, w \in \mathbb{C}^m$. Partition these vectors compatibly with the block structure, e.g., $b = \begin{bmatrix} b_1 \\ b_2 \end{bmatrix}$ with $b_1 \in \mathbb{C}^{m_1}$ and $b_2 \in \mathbb{C}^{m_2}$. The power iteration is defined based on the following set of equations for some $\beta > 0$:

$$\beta a = Mb \tag{17a}$$

$$z_1 = \frac{w_1^H a_1}{|w_1^H a_1|} w_1, \quad z_2 = \frac{\|w_2\|_2}{\|a_2\|_2} a_2 \tag{17b}$$

$$\beta w = M^H z \tag{17c}$$

$$b_1 = \frac{a_1^H w_1}{|a_1^H w_1|} a_1, \quad b_2 = \frac{\|a_2\|_2}{\|w_2\|_2} w_2. \tag{17d}$$

These equations arise from the optimality conditions for the SSV and are related to the concept of principle direction alignment (see details in Packard and Doyle^[2]). Here, we will simply show that any solution of these equations yields a lower bound on $\mu(M)$. First note that (17d) implies that $b_1 = q_1 a_1$ with $q_1 := \frac{a_1^H w_1}{|a_1^H w_1|} \in \mathbb{C}$ and $|q_1| = 1$. Equation (17d) also gives $\|b_2\|_2 = \|a_2\|_2$. Hence, there is a $Q_2 \in \mathbb{C}^{m_2 \times m_2}$ with $\bar{\sigma}(Q_2) = 1$ such that $b_2 = Q_2 a_2$. Finally, define $u := b$, $y := \beta a$ and $\Delta := \frac{1}{\beta} \text{diag}(q_1 I_{m_1}, Q_2)$. It can be verified from (17a) that $y = Mu$. Moreover, $u = \Delta y$ and $\bar{\sigma}(\Delta) = \frac{1}{\beta}$ by construction. Hence, $\Delta \in \mathbf{\Delta}$ satisfies the determinant condition and yields the lower bound $\mu(M) \geq \frac{1}{\bar{\sigma}(\Delta)} = \beta$.

The power iteration attempts to solve (17) by iterating through the various relations therein. The procedure is summarized in Algorithm 2. The algorithm, as stated, runs for a fixed number of k_m iterations. However, more advanced stopping conditions can be used, e.g., terminating when the various vectors have small updates as measured in the Euclidean norm. Although $b^{[0]}, w^{[0]}$ can be chosen randomly, a more specific choice would be to use the right singular vector associated with $\bar{\sigma} \left(D_{nr}^* M (D_{nr}^*)^{-1} \right)$, where D_{nr}^* is obtained using the standard Osborne's iterations^[13].

Algorithm 2 Lower Bound: Power Iteration

- 1: (Initialization) Choose the number of iterations k_m and set $k = 0$. Select some unit-norm vectors $b^{[0]}, w^{[0]} \in \mathbb{C}^m$ and $a^{[0]} = z^{[0]} = 0 \in \mathbb{C}^m$.
 - 2: **while** $k < k_m$ **do**
 - 3: (17a): $\beta := \|M b^{[k]}\|_2$ and $a^{[k+1]} := M b^{[k]} / \beta$.
 - 4: (17b): Use $(a^{[k+1]}, w^{[k]})$ to compute $z^{[k+1]}$.
 - 5: (17c): $\beta := \|M^H z^{[k+1]}\|_2$ and $w^{[k+1]} := M^H z^{[k+1]} / \beta$.
 - 6: (17d): Use $(a^{[k+1]}, w^{[k+1]})$ to compute $b^{[k+1]}$.
 - 7: Set $k = k + 1$.
 - 8: **end while**
 - 9: Use $a^{[k_m]}, b^{[k_m]}$ and β to compute u, y and Δ .
-

This power iteration simplifies in two special cases:

- (i) $\Delta = \mathbb{C}^{m \times m}$: As noted above, $\mu(M) = \bar{\sigma}(M)$ in this case. The power iteration relations in (17) become

$$\beta a = M b, \quad z = \frac{\|w\|_2}{\|a\|_2} a, \quad \beta w = M^H z, \quad b = \frac{\|a\|_2}{\|w\|_2} w.$$

If b and w are initialized to be unit norm, then all vectors are unit norm throughout the iteration. Hence $z = a$ and $b = w$, so the relations further simplify to

$$\beta a = M b, \quad \beta b = M^H a.$$

We can iterate on these equations starting from an initial unit norm vector b . This corresponds to the standard power iteration for computing $\bar{\sigma}(M)$.

- (ii) $m := v$ and $\Delta = \{\delta I_v : \delta \in \mathbb{C}\}$: As noted above, $\mu(M) = \rho(M)$ in this case. The power iteration relations in (17) simplify to

$$\beta a = M b, \quad z = \frac{w^H a}{|w^H a|} w, \quad \beta w = M^H z, \quad b = \frac{a^H w}{|a^H w|} a.$$

Iterating these relations yields a power iteration to find the eigenvalue corresponding to the spectral radius. The iteration also yields the corresponding right b and left z^H eigenvectors.

4.2 | Generalized Power Iteration: Repeated Complex Full-Blocks

This subsection describes a generalization of the SSV power iteration to handle repeated complex full-blocks. Again, we consider the problem with $M \in \mathbb{C}^{m \times m}$ and a structured uncertainty with one $m_1 \times m_1$ full-block repeated v times as in (4). A lower bound on $\mu(M)$ is obtained by finding $\Delta \in \mathbf{\Delta}$ and non-zero vectors $y \in \mathbb{C}^m$ and $u \in \mathbb{C}^m$ such that $y = M u$ and $u = \Delta y$.

It will be useful to define the following reshaping operation $L_{m_1} : \mathbb{C}^{v m_1} \rightarrow \mathbb{C}^{m_1 \times v}$ such that $y = [y_1^H \dots y_v^H]^H \in \mathbb{C}^{v m_1}$ maps to $L_{m_1}(y) = [y_1, \dots, y_v]$. This operation restacks the partitioned vector $y \in \mathbb{C}^{v m_1}$ into a matrix. The inverse $L_{m_1}^{-1}$ will convert the matrix back to a column vector. This notation is useful to handle matrix-vector products for $\Delta \in \mathbf{\Delta}$. Specifically, let $\Delta = I_v \otimes \Delta_1$ with $\Delta_1 \in \mathbb{C}^{m_1 \times m_1}$. The relation $u = \Delta y$ is equivalent to $L_{m_1}(u) = \Delta_1 L_{m_1}(y)$.

We need one additional operation to define the generalized power iteration. Consider vectors $a, z, b, w \in \mathbb{C}^{m_1}$. Let G be a matrix of any dimension with the following SVD:

$$G = U\Sigma V^H = [U_1 \ U_2] \begin{bmatrix} \hat{\Sigma} & 0 \\ 0 & 0 \end{bmatrix} [V_1 \ V_2]^H. \quad (18)$$

Define $\mathbf{Q}(G) := U_1 V_1^H$ and note that $\bar{\sigma}(\mathbf{Q}(G)) = 1$. The power iteration is defined based on the following set of equations for some $\beta > 0$:

$$\beta a = Mb \quad (19a)$$

$$L_{m_1}(z) = \mathbf{Q}(L_{m_1}(a)L_{m_1}(w)^H) L_{m_1}(w) \quad (19b)$$

$$\beta w = M^H z \quad (19c)$$

$$L_{m_1}(b) = \mathbf{Q}(L_{m_1}(w)L_{m_1}(a)^H) L_{m_1}(a). \quad (19d)$$

Any solution of these equations yields a lower bound on $\mu(M)$. To show this, define $u := b$, $y := \beta a$ and $\Delta := I_v \otimes \frac{1}{\beta} \mathbf{Q}(L_{m_1}(w)L_{m_1}(a)^H)$. Then (19a) and (19d) are equivalent to $y = Mu$ and $u = \Delta y$. Moreover, $\bar{\sigma}(\Delta) = \frac{1}{\beta}$ by construction. Hence $\Delta \in \mathbf{A}$ satisfies the determinant condition and yields the lower bound $\mu(M) \geq \beta$. A power iteration can be used to find a solution by iterating through equations (19a)–(19d) as outlined in Algorithm 3. Note that the comments on initialization and stopping criterion for Algorithm 2 applies for Algorithm 3 as well. In cases where the power iteration does not converge, the perturbations $\Delta_1 = I_v \otimes \mathbf{Q}(L_{m_1}(a)L_{m_1}(w)^H)$ and $\Delta_2 = I_v \otimes \mathbf{Q}(L_{m_1}(w)L_{m_1}(a)^H)$ can be used to obtain a valid lower bound as $\beta = \max(\rho(\Delta_1^H M), \rho(\Delta_2 M))$.

Algorithm 3 Lower Bound: Generalized Power Iteration

- 1: (Initialization) Choose the number of iterations k_m and set $k = 0$. Select some unit-norm vectors $b^{[0]}, w^{[0]} \in \mathbb{C}^m$ and $a^{[0]} = z^{[0]} = 0 \in \mathbb{C}^m$.
 - 2: **while** $k < k_m$ **do**
 - 3: (19a): $\beta := \|Mb^{[k]}\|_2$ and $a^{[k+1]} := Mb^{[k]}/\beta$.
 - 4: (19b): $z_L := \mathbf{Q}(L_{m_1}(a^{[k+1]})L_{m_1}(w^{[k]})^H) L_{m_1}(w^{[k]})$ and $z^{[k+1]} = L_{m_1}^{-1}(z_L)$
 - 5: (19c): $\beta := \|M^H z^{[k+1]}\|_2$ and $w^{[k+1]} := M^H z^{[k+1]}/\beta$.
 - 6: (19d): $b_L := \mathbf{Q}(L_{m_1}(w^{[k+1]})L_{m_1}(a^{[k+1]})^H) L_{m_1}(a^{[k+1]})$ and $b^{[k+1]} = L_{m_1}^{-1}(b_L)$.
 - 7: Set $k = k + 1$.
 - 8: **end while**
 - 9: Use $a^{[k_m]}, b^{[k_m]}, w^{[k_m]}$ and β to compute u , y and Δ .
-

Equations (19b) and (19c) generalize the cases in the previous subsection:

- (i) $v = 1$: In this case, the block structure (4) is just a single full-block uncertainty. The stacking operations are just $L_{m_1}(z) = z$, $L_{m_1}(a) = a$, $L_{m_1}(w) = w$, and $L_{m_1}(b) = b$. Thus, an SVD of $L_{m_1}(a)L_{m_1}(w)^H = aw^H$ is given by $U_1 = \frac{a}{\|a\|_2}$, $V_1 = \frac{w}{\|w\|_2}$, and $\hat{\Sigma} = \|a\|_2\|w\|_2$. Equation (19b) is thus equivalent to $z = \frac{\|w\|_2}{\|a\|_2}a$, which corresponds to the full-block update in (17b).
- (ii) $m_1 = 1$: In this case, the block structure (4) is a scalar uncertainty repeated v times. The stacking operations are just $L_{m_1}(z) = z^T$, $L_{m_1}(a) = a^T$, $L_{m_1}(w) = w^T$, and $L_{m_1}(b) = b^T$. Thus, the stacking operation is a transpose (but not conjugation) of the column vector to a row vector. This yields:

$$L_{m_1}(a)L_{m_1}(w)^H = a^T(w^T)^H = w^H a. \quad (20)$$

This is a scalar and an SVD of this product is given by $U_1 = \frac{w^H a}{|w^H a|}$, $V_1 = 1$, and $\hat{\Sigma} = |w^H a|$. Step (19b) is thus equivalent to $z = \frac{|w^H a|}{|w^H a|}w$. This corresponds to the repeated scalar block update in (17b).

5 | RESULTS

We consider a fluid-flow problem wherein the uncertainty has a repeated full-block structure as in (4). The SSV bounds are computed for the true uncertainty structure (i.e., $\Delta \in \Delta_r$) using the proposed methods. We compare those bounds with the ones obtained by treating the uncertainty to be non-repeating (i.e., $\Delta \in \Delta_{nr}$), which is an approximation of the true uncertainty. The motivation behind this comparison is to highlight the differences that arise due to this approximation, and how those differences can alter the subsequent interpretation of the physical system/phenomena. The algorithms used for different cases are summarized in Table 1. Furthermore, we showcase the gap between the upper and lower bounds for the two sets of results. In addition, all of the above mentioned aspects have been repeated for a simple academic example.

Table 1 Different algorithms used for the results

Uncertainty Structure	$\Delta \in \Delta_{nr}$	$\Delta \in \Delta_r$
Upper Bound Algorithm	Osborne's iteration (Section 3.1)	Method of centers (Algorithm 1)
Lower Bound Algorithm	Power iteration (Algorithm 2)	Generalized power iteration (Algorithm 3)

5.1 | Example Model-1: Incompressible Plane Couette Flow

We will demonstrate our proposed algorithms on the same spatially discretized incompressible plane Couette flow (PCF) model initially used to investigate SSV—with non-repeated full-blocks—in Liu and Gayme.^[14] PCF is a simple shear-driven flow between two parallel plates, wherein the lower plate is held stationary and the upper plate moves with a fixed speed U_∞ . The PCF example is chosen as a demonstration in this study, but the proposed methods are equally applicable to other systems where repeated full-block uncertainties arise.^[14,15,25,26]

The input-output (I/O) map of the forced perturbation dynamics about a steady baseflow is a frequency response matrix defined as

$$M = C_\nabla(\kappa_x, \kappa_z)(i\omega I_{2s} - A(\kappa_x, \kappa_z))^{-1}B(\kappa_x, \kappa_z), \quad (21)$$

where ω is the temporal frequency, κ_x and κ_z are the wavenumbers from discretization in x and z directions using Fourier modes, and $A(\kappa_x, \kappa_z, Re) \in \mathbb{C}^{2s \times 2s}$, $B(\kappa_x, \kappa_z) \in \mathbb{C}^{2s \times m}$ and $C_\nabla(\kappa_x, \kappa_z) \in \mathbb{C}^{n \times 2s}$ are the system operators, respectively. Additionally, A is a function of the Reynolds number $Re = U_\infty h/\nu$, where h is the distance between the two plates and ν is the kinematic viscosity of the fluid. Then, for $M \in \mathbb{C}^{n \times m}$, we simply have the relation $\eta = Mf$ between the system inputs ($f(y, t) \in \mathbb{C}^m$) and outputs ($\eta(y, t) \in \mathbb{C}^n$) defined as

$$f = \begin{bmatrix} f_x(y, t) \\ f_y(y, t) \\ f_z(y, t) \end{bmatrix}, \quad \eta(y, t) = \begin{bmatrix} \nabla u_x(y, t) \\ \nabla u_y(y, t) \\ \nabla u_z(y, t) \end{bmatrix},$$

where ∇ is the discrete gradient operator, u_x , u_y and u_z represent flow perturbation velocities and f_x , f_y and f_z represent input forcing, in x , y and z directions, respectively. The forcing signal f is a pseudo-linear approximation of the quadratic convective nonlinear term in the incompressible PCF model. This is given by $f = \Delta \eta$ with $\Delta = I_3 \otimes \Delta_1$, where Δ_1 is considered an unknown matrix approximation of the velocity vectors (see Liu and Gayme^[14] for more details). Therefore, the uncertainty for this system is of the form shown in (4) with a rectangular block $\Delta_1 \in \mathbb{C}^{m_1 \times n_1}$ repeated three times ($v = 3$). Thus, the SSV bounds for the PCF model indicate the sensitivity of flow at each κ_x and κ_z to this forcing, which is an indication of flow's potential for transition to turbulence.^[27] Large bound values indicate that the system in (21) has a higher tendency to transition, and vice versa, which is a consequence of a variation of the small-gain condition for structured uncertainties (see Section 2). For additional details on the model formulation and discretization, we refer the reader to prior works.^[14,28]

We will use a $50 \times 90 \times 50$ grid of $n_{\kappa_x} \times n_{\kappa_z} \times n_\omega$ to compute the SSV bounds, where n_{κ_x} , n_{κ_z} and n_ω are total grid points for κ_x , κ_z and ω , respectively. We use logarithmically spaced values $\kappa_x \in [10^{-4}, 10^{0.48}]$, $\kappa_z \in [10^{-2}, 10^{1.2}]$ and $\omega \in [-10^{0.5}, 10^{0.5}]$

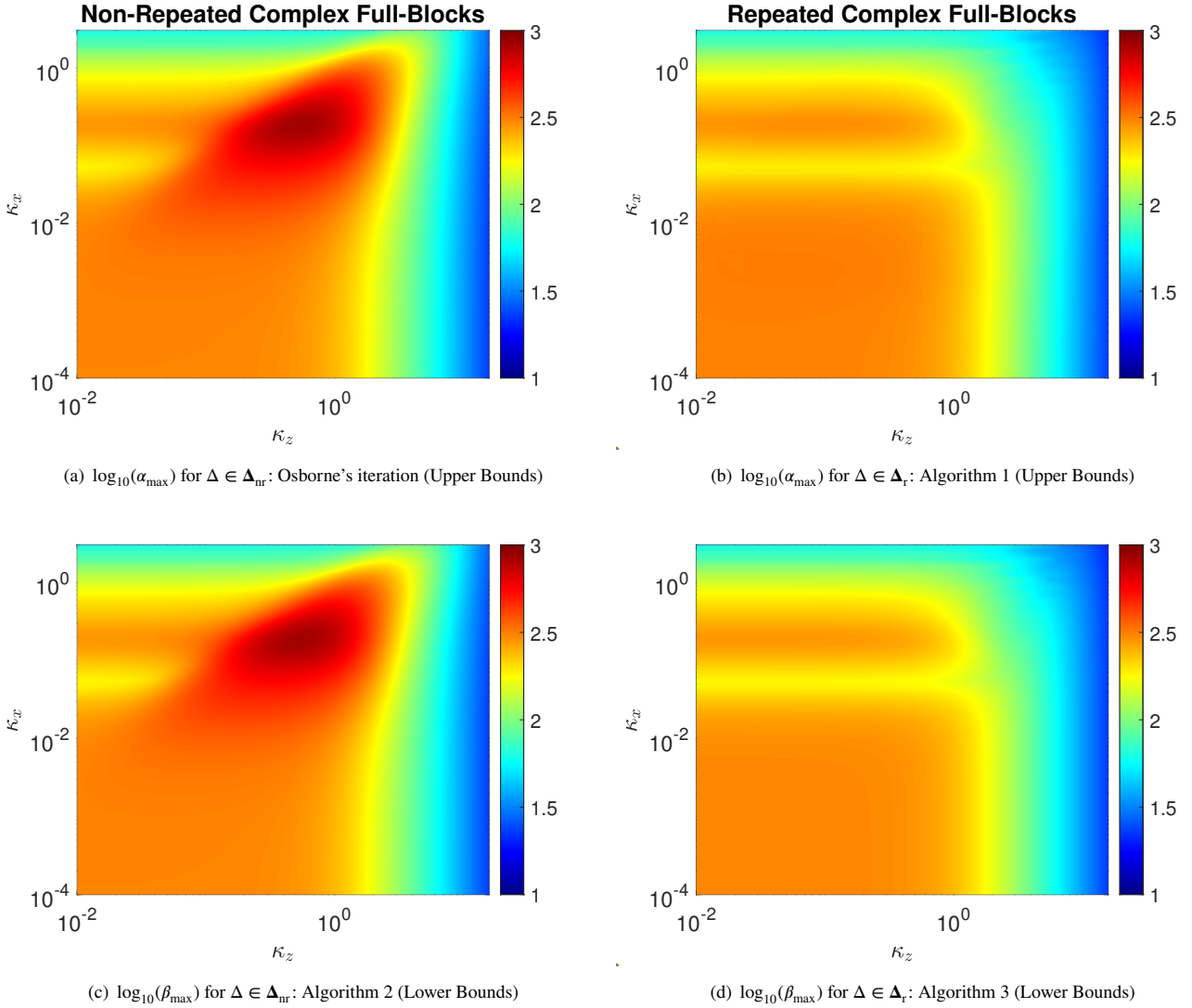


Figure 1 The α_{\max} and β_{\max} results over the wavenumber pair (κ_x, κ_z) grid. The top row plots represent the upper bounds α_{\max} and the bottom row plots represent the lower bounds β_{\max} .

for all the results in this section. Note that we consider negative temporal frequencies as the system matrices are complex-valued and the corresponding frequency response is not symmetric about the $\omega = 0$ line. The state dimension of the system is $s = 30$, and the input and output dimensions are $m = 3s = 90$ and $n = 9s = 270$, respectively. Then, $m_1 = s = 30$ and $n_1 = 3s = 90$ for Δ_1 . The operating Reynolds number for the system is set to $Re = 358$. The system is nominally stable, i.e., the eigenvalues of $A(\kappa_x, \kappa_z, Re)$ are in the open left-half plane for the parameter values chosen here. Algorithm 1 is initialized with $R = \text{diag}((d_1^*)^2, \dots, (d_v^*)^2)$ using the Osborne's iteration, $p = 1.05$, $k_m = 500$, $\theta = 10^{-3}$, $\gamma = 10^6$ and $\epsilon = 2 \times 10^{-4}$. Algorithms 2 and 3 are initialized by setting $w^{[0]}$ and $b^{[0]}$ to be the right singular vector associated with $\bar{\sigma} \left(D_{\text{nr}}^* M(i\omega) (D_{\text{nr}}^*)^{-1} \right)$, where D_{nr}^* is obtained using the standard Osborne's iterations on $M(i\omega)$. Additionally, the total number of iterations given by k_m are set to 60 for both the power iterations. Since M in (21) is a frequency response operator, we will compute the “best” upper (α_{\max}) and lower (β_{\max}) bounds at each (κ_x, κ_z) pair by choosing the maximum α and β over a spectrum of frequencies ω .

MATLAB's `parfor` command is used to compute α_{\max} and β_{\max} values using parallel computing for $n_{\kappa_x} \times n_{\kappa_z}$ grid at each n_ω . The computations were performed on a desktop computer with 3.61 GHz 12-th Gen Intel(R) Core(TM) i7-12700K processor with 12 cores and 16 GB RAM. The computation times for Algorithm 1 and Algorithm 3 were approximately 4 hours and 22

minutes, respectively. On the other hand, Osborne's iteration and Algorithm 2 took about 2 minutes and 4 minutes, respectively, to compute all the α_{\max} and β_{\max} values.

The results are depicted in Fig. 1. Comparing the results shown in Figs. 1(b) and 1(a), we deduce that α_{\max} values computed using Algorithm 1 are smaller overall than the α_{\max} values computed using the Osborne's iteration. The distributions of the α_{\max} values over the wavenumber pair grid are also markedly different. There is a prominent peak in Fig. 1(a) for the largest α_{\max} value at $\kappa_x = 0.1956$ and $\kappa_z = 0.5778$. This peak is not present in Fig. 1(b). Instead, there are two areas with similar α_{\max} values, which are separated by a narrow 'valley' in between. Therefore, approximating a repeating full-block uncertainty with a non-repeating one in this case not only leads to conservative upper bound estimates, but also results in a local maximum that does not necessarily represent actual system behavior. A similar argument follows for the lower bounds computed using the two power iteration variants, as shown in Figs. 1(c) and 1(d). Additionally, the largest α_{\max} value in Fig. 1(b) corresponds to the negative spectrum of temporal frequency grid, which provides further insight into the most sensitive direction for instability of the PCF model in (21).

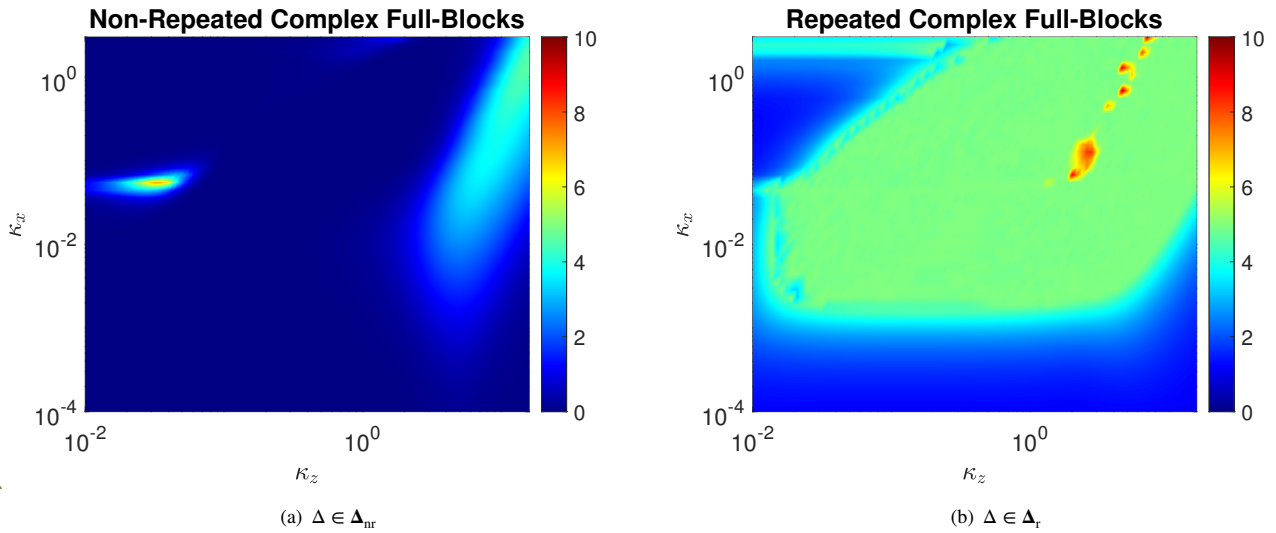


Figure 2 The percentage difference between α_{\max} and β_{\max} values over the wavenumber pair (κ_x, κ_z) grid. The stopping ratio between upper and lower bounds for Algorithm 1 was set to 1.05, which means that all the computed upper bounds must be within 5% of the lower bounds. Therefore, the majority of percentage differences in (b) are $\leq 5\%$. The only upper bounds that failed to achieve the stopping criterion are given by the red hotspots.

The gaps between α_{\max} and β_{\max} are shown in Figs. 2(a) and 2(b) which indicate that β_{\max} values are within 5% of α_{\max} values for approximately 99.8% and 98.9% of wavenumber pairs in Fig. 2(a) and Fig. 2(b), respectively. This means that the true SSV values lie within a small interval for a large subset of the wavenumber pairs considered for both repeated and non-repeated full-blocks. A summary of the gaps in both sets of bounds is provided in Table 2. Although the stopping ratio between upper and lower bounds for Algorithm 1 is set to 1.05, we still end up with a percentage difference greater than 5% at some wavenumber pairs (see Fig. 2(b)). However, the maximum gap is 9.33% for only one wavenumber pair and the rest of the wavenumber pairs have an average gap of 6.5% at the hotspots in Fig. 2(b). The relatively large gap can be attributed to one of the three reasons: (i) The D -scale upper bound is not necessarily equal to μ , (ii) the upper bound algorithm fails to converge to the optimal D -scale, and/or (iii) the power iteration fails to converge to the true value of μ . It is possible that the repeated complex full-blocks are a special case, where μ is equal to its corresponding D -scale upper bound. In this case, issue (i) would not be the source of the gap. We will explore this conjecture in future work.

To further investigate the bounds, we plot α and β over the temporal frequency at chosen wavenumber pairs (κ_x, κ_z) . These results for the non-repeated and repeated full-blocks are shown in Figs. 3 and 4, respectively. The wavenumber pairs chosen are the ones corresponding to the largest and smallest gap between α_{\max} and β_{\max} over the wavenumber pair grid. The result in

Table 2 Summary of the gaps between α_{\max} and β_{\max} for the Couette flow model

Uncertainty Structure	$\Delta \in \Delta_{nr}$	$\Delta \in \Delta_r$
Maximum gap, (κ_x, κ_z)	7.09%, (0.055, 0.032)	9.33%, (0.692, 4.578)
Minimum gap, (κ_x, κ_z)	$3.2 \times 10^{-5}\%$, (0.005, 0.011)	1.14%, (10^{-4} , $10^{1.2}$)
Average gap	0.46%	3.8%

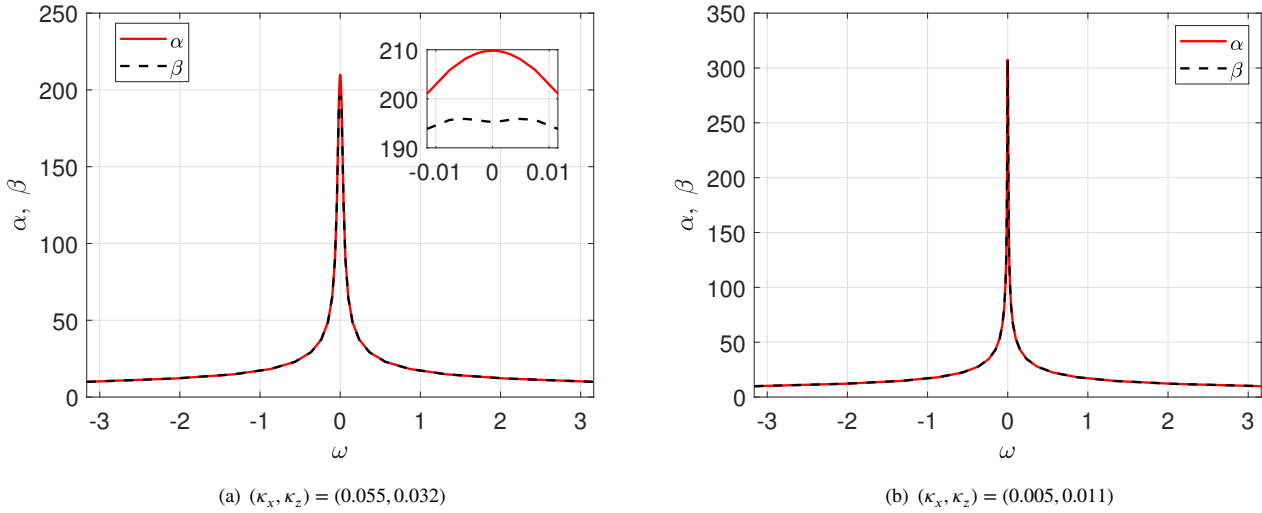
**Figure 3** The α and β results over the temporal frequency (ω) grid for $\Delta \in \Delta_{nr}$. The (a) and (b) correspond to wavenumber pairs where the gap between α_{\max} and β_{\max} are the largest and smallest, respectively.

Fig. 3(a) showcases the bounds for the non-repeated full blocks at $(\kappa_x, \kappa_z) = (0.055, 0.032)$, where the gap between α_{\max} and β_{\max} is the largest at 7.09%. The zoomed-in plot in Fig. 3(a) highlights a single global peak in α at $\omega \approx 0$, while there are two local peaks in β , located almost symmetrically about the $\omega = 0$ line at $\omega = \pm 0.005$. In the case of smallest gap between α_{\max} and β_{\max} for the non-repeated full-blocks, which occurs at $(\kappa_x, \kappa_z) = (0.005, 0.011)$, the bounds are virtually identical (see Fig. 3(b)). On the other hand, both the bounds are qualitatively similar for the repeated full-blocks case, as shown in Fig. 4. The largest gap between α_{\max} and β_{\max} in this case occurs at $(\kappa_x, \kappa_z) = (0.692, 4.578)$, and both α and β have two local peaks that occur at $\omega = \pm 0.365$ (see Fig. 4(a)). Although these peaks are symmetric about the $\omega = 0$ line, the peak α values in Fig. 4(a) at $\omega = -0.365$ and $\omega = 0.365$ are 56.799 and 56.651, respectively.

5.2 | Simple Academic Example

We now demonstrate the proposed algorithms on a MIMO LTI system with the frequency response matrix given by $M = C(i\omega I_4 - A)^{-1}B$, where ω is the temporal frequency and the randomly generated state-space matrices $A, B, C \in \mathbb{C}^{4 \times 4}$ are as follows:

$$A = \begin{bmatrix} 0.720 - i0.663 & -0.602 - i0.684 & -1.937 - i0.792 & -1.021 - i0.153 \\ 0.059 - i1.875 & -1.103 + i0.350 & -0.728 + i0.164 & -0.135 + i2.021 \\ 0.071 + i0.114 & 0.948 + i0.237 & -1.493 + i0.491 & 1.486 - i0.025 \\ -0.647 - i0.260 & -0.272 + i0.829 & -0.709 + i0.908 & -0.506 + i0.276 \end{bmatrix},$$

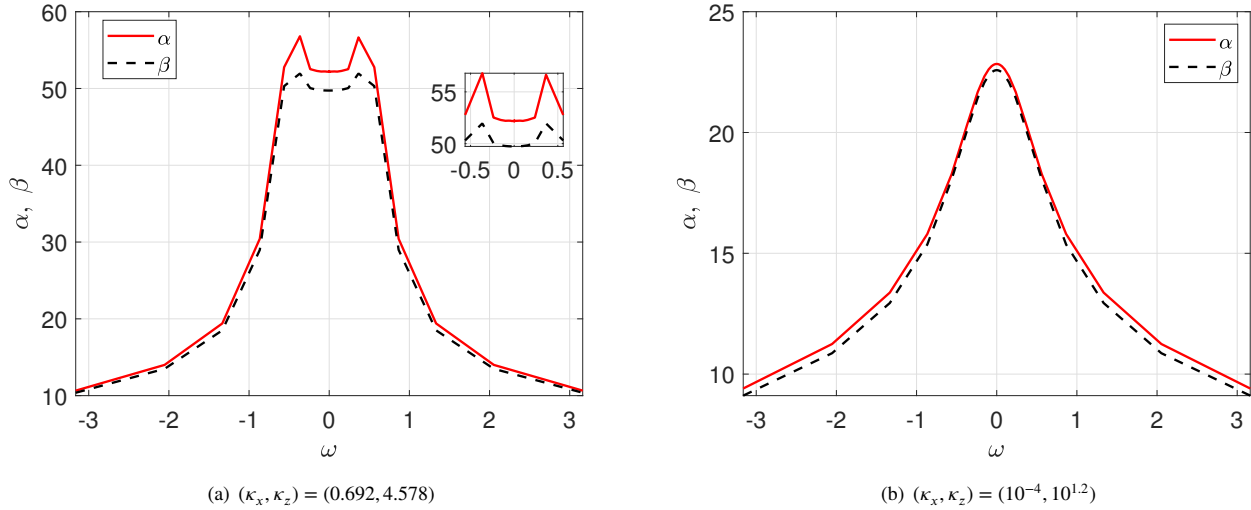


Figure 4 The α and β results over the temporal frequency (ω) grid for $\Delta \in \Delta_1$. The (a) and (b) correspond to wavenumber pairs where the gap between α_{\max} and β_{\max} are the largest and smallest, respectively.

$$B = \begin{bmatrix} 0.738 - i0.773 & 1.271 + i0.118 & 1.152 + i0.494 & -0.764 - i0.400 \\ -0.166 + i0.896 & 0.504 + i1.761 & 0.291 - i0.516 & 0.425 - i0.028 \\ -1.103 + i0.449 & -1.408 - i0.195 & 0.067 - i1.287 & -0.595 + i0.316 \\ 1.308 - i0.744 & 0.358 + i0.728 & -0.174 + i0.665 & -1.489 - i0.094 \end{bmatrix},$$

$$C = \begin{bmatrix} 0.255 + i0.101 & 1.681 + i0.048 & -0.386 - i0.051 & 0.633 - i0.874 \\ -1.827 + i1.132 & -0.267 - i0.846 & -0.863 + i0.840 & 0.244 + i1.447 \\ 1.877 + i0.179 & -1.124 + i0.752 & 1.014 + i0.731 & -1.502 + i0.431 \\ -0.803 + i1.056 & 0.002 - i0.284 & 1.029 - i0.801 & -0.444 + i0.543 \end{bmatrix}.$$

The nominal system is stable as all the eigenvalues of A are in the open left-half plane. The uncertainty for this model is chosen as $\Delta = I_2 \otimes \Delta_1$ with $\Delta_1 \in \mathbb{C}^{2 \times 2}$. Numerical implementation of the algorithms are as described in Section 5.1. We take 200 logarithmically spaced points for $\omega \in [-10^{1.5}, 10^{1.5}]$. The results for α and β for both the non-repeated and repeated cases are shown in Fig. 5. In terms of qualitative similarities, there are two peaks—one for $\omega < 0$ and the other for $\omega > 0$ —in each bound in both the cases, and the bounds are not symmetric about the $\omega = 0$ line. However, approximating the repeated full-block structure with a non-repeated one leads to very conservative bounds at some temporal frequencies. For example, the α value in Fig. 5(a) is approximately 1.7 times that of the α value in Fig. 5(b) at $\omega = 1.896$. A similar set of comments applies to the lower bounds β at $\omega = 1.896$. This means that the true value of μ at this frequency in the non-repeated case is roughly 1.7 times that of the repeated case. It is also noteworthy that the global peaks of the bounds in Fig. 5(a) are at $\omega > 0$, whereas the global peaks in Fig. 5(b) are at $\omega < 0$. Therefore, similar to the fluid-flow example, neglecting the repeated structure of the uncertainty can not only lead to conservative bounds, which translates into conservative stability-margin estimates, but also might lead to inaccurate conclusions about the temporal behavior of the system.

6 | CONCLUSIONS

We proposed two algorithms for computing upper and lower bounds of structured singular value for repeated complex full-block uncertainty. Such uncertainty structures naturally arise in models of fluid flows and other convective systems. The proposed algorithms yield bounds that are less conservative as compared to the algorithms that ignore the repeated full-block structure, e.g., Osborne's iteration for non-repeated full-blocks. Thus, properly accounting for the repeated block structure can improve stability-margin estimates and also enable one to draw more representative conclusions regarding the temporal behavior of

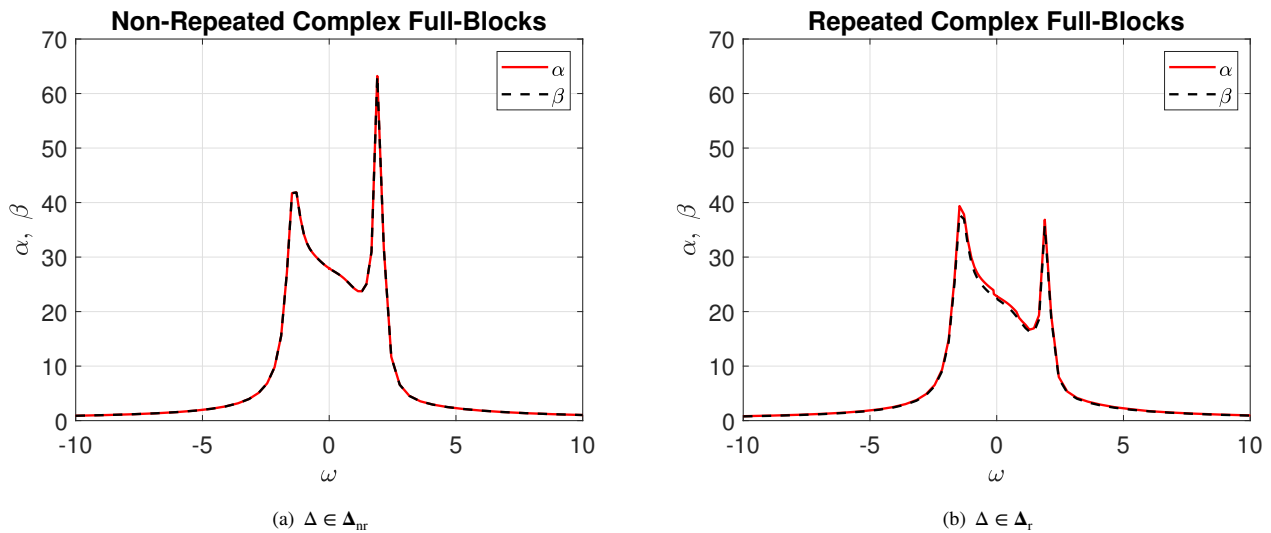


Figure 5 The α and β results over the temporal frequency (ω) grid. Although we consider $\omega \in [-10^{1.5}, 10^{1.5}]$, the results are shown for $\omega \in [-10, 10]$ to better highlight the local behavior of the bounds.

the system. These points were demonstrated on an example of incompressible plane Couette flow and an academic example. Furthermore, our future work will involve investigating the gap between the μ and the convex (or D -scale) upper bound for a single repeated full-block. This particular case is of interest due to the fact that μ is equal to its upper bound for a single full block and also for a single repeated complex scalar.

ACKNOWLEDGEMENTS

This material is based upon work supported by the Air Force Office of Scientific Research under award number FA9550-21-1-0106, the Army Research Office under award number W911NF-20-1-0156, the National Science Foundation under award number CBET-1943988, and the Office of Naval Research under award number N00014-22-1-2029.

References

1. Doyle J. Analysis of feedback systems with structured uncertainties. In: IEE Proceedings D (Control Theory and Applications). ; 1982: 242–250
2. Packard A, Doyle J. The complex structured singular value. *Automatica* 1993; 29(1): 71–109. doi: 10.1016/0005-1098(93)90175-S
3. Safonov MG. Stability margins of diagonally perturbed multivariable feedback systems. In: 20th IEEE Conference on Decision and Control including the Symposium on Adaptive Processes. ; 1981: 1472-1478
4. Zhou K, Doyle J, Glover K. *Robust and Optimal Control*. Feher/Prentice Hall Digital and Prentice Hall . 1996.
5. Dullerud GE, Paganini F. *A course in robust control theory: a convex approach*. 36. Springer Science & Business Media . 2013.
6. Braatz RP, Young PM, Doyle JC, Morari M. Computational complexity of μ calculation. *IEEE Transactions on Automatic Control* 1994; 39(5): 1000–1002. doi: 10.1109/9.284879

7. Demmel J. The Componentwise Distance to the Nearest Singular Matrix. *SIAM J. Matrix Anal. Appl.* 1992; 13(1): 10-19. doi: 10.1137/0613003
8. Young P, Doyle J. Computation of μ with real and complex uncertainties. In: 29th IEEE Conference on Decision and Control. ; 1990: 1230-1235 vol.3
9. Young PM, Newlin MP, Doyle JC. Practical computation of the mixed μ problem. In: American Control Conference. ; 1992: 2190-2194
10. Troeng O. Five-Full-Block Structured Singular Values of Real Matrices Equal Their Upper Bounds. *IEEE Control Systems Letters* 2021; 5(2): 583-586. doi: 10.1109/LCSYS.2020.3004297
11. Colombino M, Smith RS. A Convex Characterization of Robust Stability for Positive and Positively Dominated Linear Systems. *IEEE Transactions on Automatic Control* 2016; 61(7): 1965-1971. doi: 10.1109/TAC.2015.2480549
12. Fan M, Tits A, Doyle J. Robustness in the presence of mixed parametric uncertainty and unmodeled dynamics. *IEEE Transactions on Automatic Control* 1991; 36(1): 25-38. doi: 10.1109/9.62265
13. Packard A, Fan M, Doyle J. A power method for the structured singular value. In: 27th IEEE Conference on Decision and Control. ; 1988: 2132-2137 vol.3.
14. Liu C, Gayme DF. Structured input–output analysis of transitional wall-bounded flows. *Journal of Fluid Mechanics* 2021; 927. doi: 10.1017/jfm.2021.762
15. Liu C, Colm-cille PC, Gayme DF. Structured input–output analysis of stably stratified plane Couette flow. *Journal of Fluid Mechanics* 2022; 948: A10. doi: 10.1017/jfm.2022.648
16. Liu C, Shuai Y, Rath A, Gayme DF. A structured input-output approach to characterizing optimal perturbations in wall-bounded shear flows. In: American Control Conference. ; 2023: 2319-2325
17. Bhattacharjee D, Mushtaq T, Seiler PJ, Hemati M. Structured Input-Output Analysis of Compressible Plane Couette Flow. In: AIAA SCITECH FORUM. ; 2023: 1984
18. Balas G, Chiang R, Packard A, Safonov M. Robust control toolbox user’s guide. *The Math Works, Inc., Tech. Rep* 2007.
19. Boyd S, El Ghaoui L. Method of centers for minimizing generalized eigenvalues. *Linear Algebra and its Applications* 1993; 188-189: 63-111. doi: [https://doi.org/10.1016/0024-3795\(93\)90465-Z](https://doi.org/10.1016/0024-3795(93)90465-Z)
20. Boyd S, El Ghaoui L, Feron E, Balakrishnan V. *Linear Matrix Inequalities in System and Control Theory*. Society for Industrial and Applied Mathematics . 1994
21. Safonov MG. *Stability and Robustness of Multivariable Feedback Systems*. MIT press . 1980.
22. Nesterov YE, Nemirovskii A. An interior-point method for generalized linear-fractional programming. *Mathematical Programming* 1995; 69(1): 177–204. doi: 10.1007/BF01585557
23. Mehrotra S. On the Implementation of a Primal-Dual Interior Point Method. *SIAM Journal on Optimization* 1992; 2(4): 575-601. doi: 10.1137/0802028
24. Osborne EE. On Pre-Conditioning of Matrices. *Journal of the ACM* 1960; 7(4): 338–345. doi: 10.1145/321043.321048
25. McKeob BJ, Sharma AS. A critical-layer framework for turbulent pipe flow. *Journal of Fluid Mechanics* 2010; 658: 336–382. doi: 10.1017/S002211201000176X
26. Chavarin A, Luhar M. Resolvent Analysis for Turbulent Channel Flow with Riblets. *AIAA Journal* 2020; 58(2): 589-599. doi: 10.2514/1.J058205
27. Liu C, Gayme DF. Input-output inspired method for permissible perturbation amplitude of transitional wall-bounded shear flows. *Phys. Rev. E* 2020; 102: 063108. doi: 10.1103/PhysRevE.102.063108

28. Jovanović MR, Bamieh B. Componentwise energy amplification in channel flows. *Journal of Fluid Mechanics* 2005; 534: 145-183. doi: 10.1017/S0022112005004295
29. Boyd S, Vandenberghe L. *Convex Optimization*. Cambridge University Press . 2004.

How to cite this article: Talha Mushtaq, Diganta Bhattacharjee, Peter Seiler, and Maziar S. Hemati (2023), Structured Singular Value of a Repeated Complex Full-Block Uncertainty, *Int J Robust Nonlinear Control*. <year> <vol> Page <xxx>-<xxx>

APPENDIX

A GENERALIZED OSBORNE

In this section, we will describe a fast algorithm for $\Delta \in \mathbf{\Delta}_r$ and $M \in \mathbb{C}^{m \times m}$. The standard Osborne iteration cannot be used for $\mathbf{\Delta}_r$ as $D \in \mathbf{D}_r$ contains off-diagonal entries. This section describes our generalization of Osborne's method (GenOsborne) to handle the matrix scales in (7). The proposed GenOsborne algorithm is an iteration that solves the following minimization problem:

$$\min_{D \in \mathbf{D}_r} \|DM D^{-1}\|_F^2 \quad (\text{A1})$$

where \mathbf{D}_r is defined in (7). To simplify the calculations, we use the square of Frobenius norm in (A1). Let s_{ij} denote the (i, j) entry of S in (7). The Frobenius norm in (A1) yields a cumbersome expression that has various $s_{ij} \in \mathbb{C}$ entries multiplying each other. Thus, it is difficult to minimize the function for each s_{ij} , since each of the scalings are coupled together. To avoid this issue, we iteratively optimize over a single off-diagonal entry and then couple it, similar to the Osborne's iteration. Thus, we first use the standard Osborne's iterations to calculate the optimal diagonal scalings s_i^* and then use an iterative approach to optimize a single off-diagonal term $s_{ij} \in \mathbb{C}$ at each iteration and iterate over all possible pairs of (i, j) , where $i \neq j$. We denote the matrices with a single off-diagonal entry $s_{ij} \in \mathbb{C}$ as $D_{ij} = S_{ij} \otimes I_{m_1}$, where S_{ij} has ones along the diagonal, s_{ij} in the (i, j) entry and zero everywhere else.

Let $M^{[k]}$ be the scaled matrix at step k of the generalized iteration and $s_{ij} \in \mathbb{C}$ be the off-diagonal scaling to be optimized. Then, the objective function is:

$$\begin{aligned} f_1(s_{ij}) &= \|D_{ij} M^{[k]} D_{ij}^{-1}\|_F^2 \\ &= c_0 + \text{conj}(c_1 s_{ij}) + c_1 s_{ij} + c_2 \|s_{ij}\|^2 + c_3 s_{ij}^2 \\ &\quad + \text{conj}(c_3) (\text{conj}(s_{ij}))^2 + c_4 s_{ij}^2 (\text{conj}(s_{ij})) \\ &\quad + \text{conj}(c_4) s_{ij} (\text{conj}(s_{ij}))^2 + c_5 \|s_{ij}^2\|^2 \end{aligned} \quad (\text{A2})$$

where $\{c_0, \dots, c_5\} \subseteq \mathbb{C}$ are coefficients that can be computed from the definition of the Frobenius norm. Note that the coefficients depend on the pair (i, j) and $M^{[k]}$. By expressing $s_{ij} = s_{R_{ij}} + i s_{I_{ij}}$, the objective function $f_1(s_{ij})$ can be written in the following equivalent form:

$$\begin{aligned} f_2(\bar{s}_{ij}) &= c_0 + 2\text{Re}(c_1) s_{R_{ij}} - 2\text{Im}(c_1) s_{I_{ij}} \\ &\quad + (c_2 + 2\text{Re}(c_3)) s_{R_{ij}}^2 + (c_2 - 2\text{Re}(c_3)) s_{I_{ij}}^2 \\ &\quad - 4\text{Im}(c_3) s_{R_{ij}} s_{I_{ij}} + 2\text{Re}(c_4) s_{R_{ij}} (s_{R_{ij}}^2 + s_{I_{ij}}^2) \\ &\quad - 2\text{Im}(c_4) s_{I_{ij}} (s_{R_{ij}}^2 + s_{I_{ij}}^2) + c_5 (s_{R_{ij}}^2 + s_{I_{ij}}^2)^2 \end{aligned} \quad (\text{A3})$$

where $\bar{s}_{ij} = [s_{R_{ij}}, s_{I_{ij}}]^T$. We use the damped newton method (see Algorithm 9.5 in Boyd and Vandenberghe^[29]) to solve the minimization problem. Therefore, we obtain the local optimum $\bar{s}_{ij}^* = \text{argmin}_{\bar{s}_{ij} \in \mathbb{R}^2} f_2(\bar{s}_{ij})^2$. Hence, each $s_{ij}^* = s_{R_{ij}}^* + i s_{I_{ij}}^*$ has the corresponding scaling matrix D_{ij}^* . We perform the following update for $k \geq 1$:

$$M^{[k+1]} = D_{ij}^* M^{[k]} (D_{ij}^*)^{-1}. \quad (\text{A4})$$

² $f_2(\bar{s}_{ij})$ is non-convex for some combinations of the coefficients $\{c_0, \dots, c_5\}$. Therefore, the solution is only guaranteed to converge to a local optimum.

The iterative algorithm results in the total effective scaling as:

$$D'' = \left(\prod_{\forall i,j,i \neq j} D_{ij}^* \right) D_{nr}^* \quad (A5)$$

where D_{nr}^* is the optimal diagonal scaling after applying the standard Osborne's iteration. For example, if we choose to optimize the s_{12} entry then we compute s_{12} by minimizing (A3). We scale the matrix $M^{[2]} = D_{12}^* M^{[1]} (D_{12}^*)^{-1}$, where $M^{[1]} = D_{nr}^* M (D_{nr}^*)^{-1}$. We use $M^{[2]}$ and repeat the steps for other s_{ij} until all s_{ij} are computed and effectively D'' is obtained. The above approach allows for computing optimal value of each s_{ij} and then coupling them. Finally, the upper bound is computed as $\alpha = \bar{\sigma}(D'' M (D'')^{-1})$. We refer to the entire process of computing D'' described above as the Generalized Osborne algorithm or GenOsborne for short, which is summarized in Algorithm 4.

Algorithm 4 Upper Bound: GenOsborne Algorithm

- 1: (Initialization) Use the standard Osborne's method on M to obtain the diagonal scaling matrix D_{nr}^* . Define $M^{[1]} = D_{nr}^* M (D_{nr}^*)^{-1}$. Set $k = 1$.
 - 2: **for** $k = 1$ to $v(v-1)$ **do**
 - 3: Set (i, j)
 - 4: Compute coefficients $\{c_e\}_{e=0}^5$ for (i, j) and $M^{[k]}$.
 - 5: Find $\bar{s}_{ij}^* = \operatorname{argmin}_{\bar{s}_{ij} \in \mathbb{R}^2} f_2(\bar{s}_{ij})$ using the damped newton method and form $s_{ij}^* = s_{R_{ij}}^* + i s_{I_{ij}}^*$ from \bar{s}_{ij}^* .
 - 6: Compute the corresponding D_{ij}^* and set $M^{[k+1]} = D_{ij}^* M^{[k]} (D_{ij}^*)^{-1}$,
 - 7: **end for**
 - 8: Compute the upper bound $\alpha = \bar{\sigma}(M^{[k]})$
-